"Trinity" CT Architecture – A Stationary CT System

Qingsong Yang, Lars Gjesteby, Wenxiang Cong, Dan Harrison and Ge Wang*
Department of Biomedical Engineering
Rensselaer Polytechnic Institute,
Troy, NY, 12180, USA
Wangg6@rpi.edu

Mark Eaton
Stellarray, Inc., 9210 Cameron Road,
Suite 300,
Austin, TX, 78754, USA
eaton@stellar-micro.com

Mark B. Williams
Department of Radiology and Medical Imaging,
University of Virginia,
Charlottesville, VA22908, USA
mbwilliams@virginia.edu

***Abstract* — Since the temporal resolution of a CT scanner is mainly limited by the rotation speed of the CT gantry, we are motivated to remove any mechanical rotation and achieve a completely stationary architecture. For fast cardiac imaging, in particular, we propose a "Trinity" CT architecture with three linear/curvilinear x-ray source arrays, each paired with an opposing 2D detector array. In this proposed design, the x-ray source arrays and associated detector arrays are arranged in a hexagon around the object to be scanned. Data collected in this geometry are truncated to various degrees and, to perform image reconstruction, an iterative algorithm is developed and implemented in the compressed-sensing framework. Numerical simulation suggests that this system architecture yields good quality reconstructions over a large field of view, with even better quality within smaller interior regions of interest. Relevant issues are also discussed for further research.**

Keywords — X-ray CT, stationary gantry, ROI reconstruction, compressed sensing.

I. INTRODUCTION

According to the World Health Organization, cardiovascular disease (CVD) is the number one cause of death globally. Around 17.5 million people died from CVDs in 2012 [1]. Given the global prevalence, a powerful imaging tool is needed for early detection of cardiac disease before symptom presentation.

X-ray computed tomography (CT) is one of the most popular imaging tools for cardiac disease detection and characterization [2, 3]. Temporal resolution is a very important aspect of cardiac imaging. Insufficient data acquisition speed can cause image artifacts that deform important features and compromise diagnosis. In order to increase CT temporal resolution, dual-source technology has been used for medical CT [2, 3]. Theoretically, triple source CT can increase temporal resolution by a factor of three [4, 5]. Moreover, large cone-angle CT also improves temporal resolution, compared to conventional narrow-angle CT, because it reduces the time needed to scan in the z direction [6]. An example is the Aquilion ONE 320-row multi-slice CT scanner (Toshiba Medical Systems Corporation, Japan), allowing a 16 cm z-coverage within a sub-second scan [7].

Despite the development of fast CT systems, the rotation speed of the CT gantry remains a limiting aspect of temporal resolution. Accordingly, stationary CT systems not requiring physical motion of the x-ray tube continue to be of interest. The electron beam CT (EBCT) was the earliest stationary CT system [8, 9]. Similarly, an electron beam micro-CT (EBMCT) was proposed for dynamic small-animal imaging [10]. EBCT uses a ring-shaped anode encircling the subject to generate a rapidly moving x-ray focal spot by electromagnetically steering an electron beam to different locations on the anode. Also, investigators at the Mayo Clinic developed a dynamic spatial reconstructor (DSR) [11] that utilizes an array of x-ray sources on a semi-circle and an array of detectors on an opposing semi-circle. More recently, x-ray sources based on carbon nanotube (CNT) cold cathodes were developed that are compact and can be rapidly switched on and off [12]. A stationary micro-CT system was proposed using an array of CNT sources in an arrangement similar to that of the DSR [13]. These and other recently developed digitally controlled cold-cathode x-ray sources promise dramatic CT temporal resolution improvement due to their microsecond switching speeds and configurability as stationary multi-spot arrays [12, 14].

In an initial effort, we here consider and simulate a stationary CT system we call Trinity that is equipped with three cold-cathode multi-spot arrays, each with an associated spatially opposing detector array. The Trinity system has potential to achieve high temporal resolution while collecting scan data symmetrically from three orientations spaced by 120 degrees. The rest of this paper is organized as follows. In section 2, we describe the Trinity system architecture and an associated reconstruction algorithm. In section 3, we present results from numerical simulations that demonstrate the potential capability of this system. In the final section, we discuss related issues and draw conclusions.

II. METHODOLOGY

A. System Architecture & Cold-Cathode X-ray Source Technology

The proposed preclinical CT system is shown using compact x-ray sources and flat-panel detectors in Figure 1. The system can be operated with a small region-of-interest (ROI), e.g. for cardiac imaging, or with a wider field of view, e.g. for whole-animal imaging. With the inherently fast switching times of the cold cathodes and with appropriate pre-detector collimation,

DOI: 10.12059/Fully3D.2017-11-3203004

several source spots can be active in each source array at any given time. For example, with three source arrays and each array having 4 source spots simultaneously active, scan times may be reduced by a factor of 12. Scanning is achieved by sequencing through and activating the source spots comprising each array. The animal or phantom would be completely stationary.

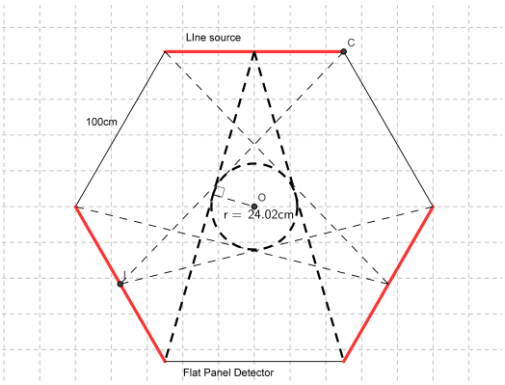

Figure 1. 2D view of the "Trinity" preclinical CT system architecture. The red lines represent the three arrays of x-ray focal spots, and the black lines represent the corresponding detector arrays.

X-rays are generated when electrons from each cold-cathode are accelerated and strike the anode. The resulting x-ray focal spot can be independently controlled through digital control of the associated cold-cathode field-emission gate. Source collimators are needed at the exit surface of each source array to confine the x-ray beams to the opposing detector surface, and each source array must be specially designed to minimize dead spaces at source-detector junctions. The sources developed by Stellarray, for example, have insulating source sidewalls so they can be placed directly against or slightly in front of the adjacent detectors.

Successful development of a cold-cathode source array has significant challenges. Cold cathodes require a high-quality vacuum, on the order of 10^{-7} Torr or better, for long life. To keep the system compact, vacuum pumps can be avoided by permanently sealing the source-array container after sufficient cleansing, baking and pumping to create the high vacuum. Furthermore, materials used in the source must have closely matched coefficients of thermal expansion (CTE) since the source must be baked out at high temperature to ensure good internal vacuum. In operation, "getters" are used to absorb stray gasses, but with current CNT technology, some will still emit enough gas or particulate debris to degrade the vacuum.

An alternative cold-cathode technology under development is an innovative "triple point" (TP) cold cathode made by depositing multiple alternating conductive and insulating thin films (~ 100Å) on insulating substrates or on thin metal ribbons or wires. These structures them become cold-cathode "edge" emitters when facing a vacuum. These have acceptable outgassing characteristics but also have a high degree of E-field enhancement that yields good cathode (electron emission) performance. Field enhancement in cold cathodes can be provided by insuring a large aspect ratio of the emitter (tall tips, thin edges). This is provided with TPs by the intersection of the very thin conductor and insulator layers within the vacuum.

A high voltage is needed between the cold cathode and the anode in order to accelerate the emitted electrons toward the anode target. To make the sources more compact, the high-voltage generator can be integrated with the source array. This would eliminate the bulky high voltage cables. Finally, the vacuum package materials should be chosen to transfer heat away from the electron-beam impact spots on the anode as efficiently as possible. In Stellarray's sources, the anode can comprise or be attached to a broad metal plate that forms part of the vacuum enclosure. This metal can then be efficiently cooled by ambient air or other external means. In this case the anode would be at ground potential and the cathodes would be at a high negative potential.

An interesting possibility is to perform multi-energy imaging with our proposed architecture. Different metal types will provide some different filtrations as the x-rays leave the metal anode, but this will generally not generate a significant spectral difference. Different filters can be put in the x-ray exit path from the different anode strips to filter x-rays for various beam qualities. Different cathodes can be also held at different voltages with respect to the grounded anode, or the cathode kVp can be switched for different x-ray spectra.

B. Image Reconstruction

In the proposed CT system, the data acquired are incomplete. As seen in Figure 2, we can sort the scan data into a parallel projection sinogram that shows there are projection angles (a.k.a. "gantry angles") where a full-width projection is not obtained. Thus, reconstruction using traditional filtered back-projection (FBP) cannot produce artifact-free images. To solve the data truncation and limited angle issues, we designed and implemented an SART-TV algorithm to reconstruct an image from simulated scan data via compressed sensing [15].

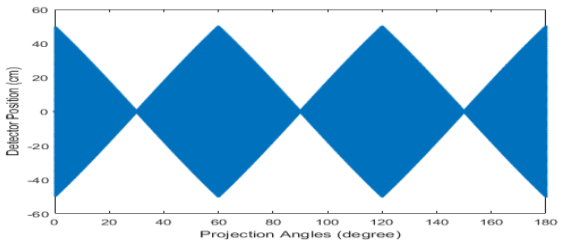

Figure 2. Re-binned parallel projection sinogram activity map for the proposed Trinity system. The blue regions (triangles and parallelograms) are measurable by the source/detector pairs. Data in the white areas are missing. Note that the vertical axis represents the detector coverage.

C. Dynamic Anti-scattering Grating

Current medical CT systems suffer from x-ray scatter that reduces image quality by adding noise and corrupting CT numbers. In conventional rotating systems, the source spot is fixed relative to the detector array and a source-focused anti-scatter grid is placed between the patient and detector to reduce the number of scattered x-ray photons that reach the detector. In order to block scattered photons in the Trinity system where the source spot is rapidly moved relative to the detector array, we propose an anti-scattering grid (pre-patient collimator) consisting of multi-layer gratings that can be rapidly moved via piezoelectric control. Figure 3 shows a two-layer grating design that we simulate in part B of section 3 for our pilot study. As the x-ray source spot is horizontally steered, the gratings are accordingly shifted so that the grating-based collimator maintains focus on the changing x-ray source location. Parameters for the two grating layers (bar width and spacing, layer distance from the detector) were adjusted specifically to the imaging geometry.

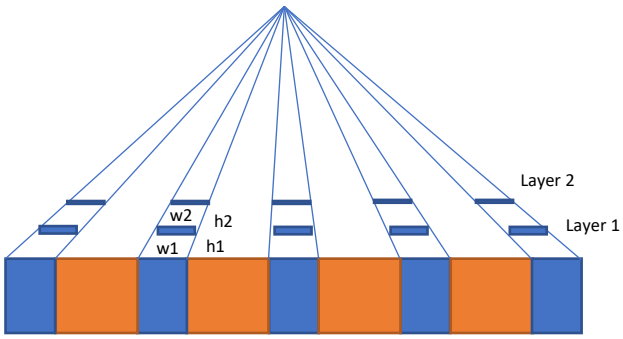

Figure 3. Simple two-layer grating-based collimator focused on one source spot to block scattering photons. The orange parts are the detector material while the blue is tungsten.

III. Numerical Simulation

A. *Image Reconstruction*

To evaluate the proposed system architecture and reconstruction algorithm, we performed a 2D numerical simulation with a modified Shepp-Logan phantom and using the geometry in Figure 1. For this pilot study, scatter was ignored. An infinite X-ray intensity (no Poisson noise) and a monochromatic source were assumed. In each x-ray source array, there were 100 perfect-point x-ray focal spots, thus 300 x-ray source positions in total. Each corresponding detector array contained 200 detector bins, each 1 mm wide, for 600 bins. A 40 x 40 cm square field of view was set into a 512x512 reconstruction grid. The reconstructed image was compared to the true phantom in Figure 4. In Figure 5, the vertical profiles are shown through the center of the true and reconstructed images of Figure 4.

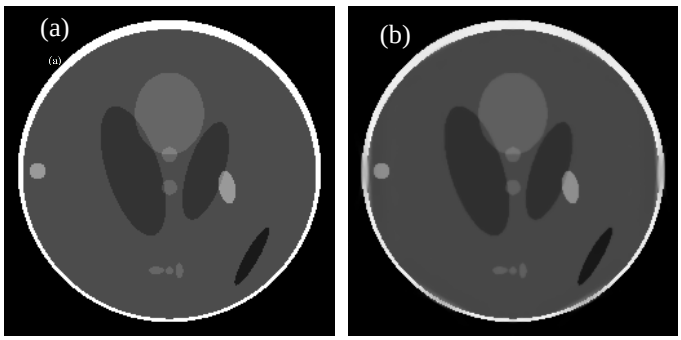

Figure 4. Numerical simulation with a modified Shepp-Logan phantom. (a) The truth and (b) the reconstruction. The display window is [0, 1].

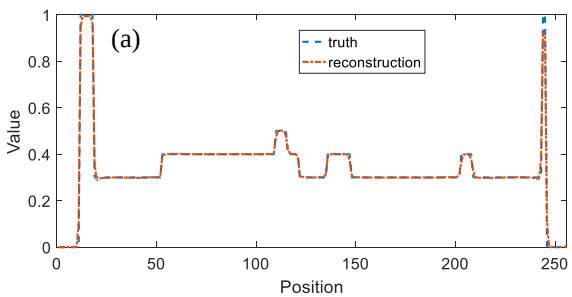

Figure 5. Vertical profile comparisons through the center of the true and reconstructed images.

We also simulated system performance using a human CT phantom that was scaled to the same size as the Shepp-Logan phantom. The result is shown in Figure 6.

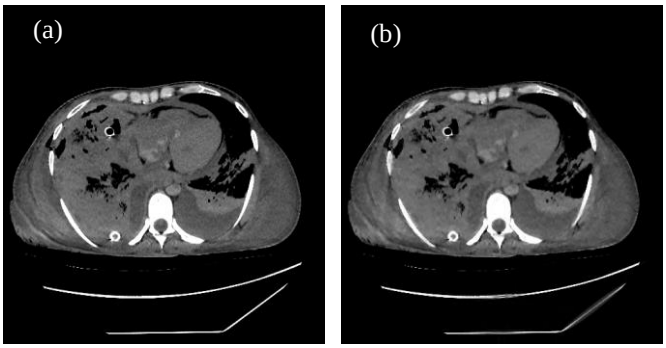

Figure 6. Numerical simulation with a human chest phantom. (a) The truth and (b) the reconstruction.

B. *Monte-Carlo Scattering Simulation*

To get an indication of the performance of a grating-based anti-scatter collimator, we performed a single-view Monte-Carlo scatter simulation using MCMP6 with a single source spot, a cylindrical water phantom, a two-layer grating-based collimator, and a detector array as shown in Figure 3. The detector array has 200 high-purity Germanium pixels that are each 0.3 cm wide and are separated by 0.2 cm Tungsten blocks. The distance between the two layers was 0.1 cm. The x-ray source was 173.2cm from the detector array and, for simplicity, an 80 keV mono-energetic x-ray source was assumed. The gratings were both 0.1 cm thick and the grating-bar widths were 0.1999cm and 0.1997cm for Layers 1 and 2 respectively (i.e., to focus on the source). The water phantom was 20 cm in diameter and was centered at the system iso-center. The source emitted 10^{10} photons in the angle spanned by each detector pixel (as would be measured by a simulated air shot). MCNP6 tracks each photon and simulates its propagation through or interaction with the phantom. Dominant Interactions, when they occur, are Compton scatter and Photoelectric absorption. As output, MCNP6 counted the surface flux at the detector block.

We simulated the following four experiments: 1) no-gratings air shot; 2) no-gratings phantom shot; 3) with-gratings air shot; 4) with-gratings phantom shot. From these data, we can calculate the Scatter-to-Primary ratio (SPR) for both the no-gratings and with-gratings experiments. The results are shown in Figure 7 where the horizontal axis is pixel index and the vertical axis is SPR.

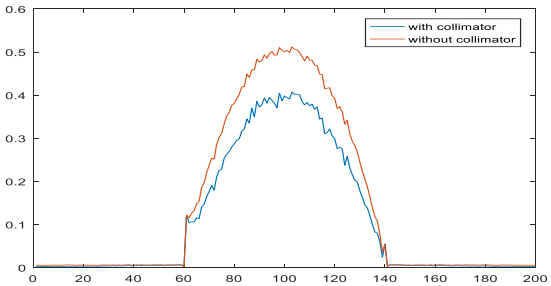

Figure 7. Scatter-to-Primary ratios with and without the two-layer grating-based collimator.

IV. Discussion

The reconstruction results in Figures 4-6 appear very good, demonstrating that the adapted SART-TV algorithm performs well without the missing data associated with the Trinity architecture. The Monte-Carlo simulation is our initial study showing an effect of the anti-scattering grid. Although the

results are promising with an increased SPR, further efforts are needed for performance optimization. While our collimating results are promising, they are far from complete. However, our novel collimator design can work for any of Trinity's x-ray source positions and yet be as effective as a conventional focused anti-scatter collimator. In principle, we may use many thin layers of gratings and shift them synchronously via piezoelectric control so that openings of the grating assembly are dynamically focused towards a moving x-ray source focal spot. Based on our communications with industrial experts in piezoelectric control, this scheme is in principle feasible but how fast a lead collimator can be moved remains a topic for research. It should be also noted that we only simulated scattering from a single source. When three focal spots from all the three line sources are simultaneously firing, cross-scattering can be corrected using a method similar to what was described in [16].

The proposed Trinity design is different from a closely-related CNT-based CT system design reported in [13]. Geometrically, the proposed Trinity design and the prior-art CNT design differ in the projection or view-sampling pattern. In the prior-art design, the x-ray sources are placed on one side of the scan circle and the detectors are placed on the other side. Projection data collected for all source positions can then be re-binned to a parallel beam geometry. The resulting "half-scan" sinogram map is shown in Figure 8. Comparing this to the Trinity sinogram map of Figure 2, we see the "half-scan" has a wide range of projection angles where data is missing. On the other hand, the trinity map has slightly more missing data, but it is more uniformly spread across the projection- angle range.

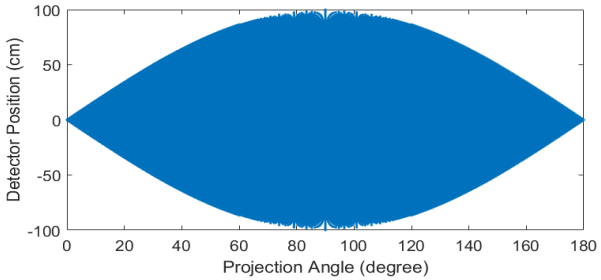

Figure 8. Rebinned sinogram coverage for the prior art "half-scan" design.

Physically, the sampling symmetry of our trinity design could have an advantage in reducing systematic biases due to beam hardening, scattering, and object asymmetry, since variations from representative orientations might tend to cancel out better than that with an asymmetric sampling pattern. For example, it is well known that CT numbers from full-scan and half-scan datasets are substantially different, and that the full-scan numbers are more reliable, while half-scan reconstruction may suffer from shading as identified in [17].

V. Conclusion

In conclusion, we have proposed a stationary CT system architecture we call Trinity. Compared to the previous work, our interlaced source-detector configuration provides angularly symmetric data acquisition and associated merits. The numerical simulation results suggest that the data collected by the trinity system are sufficient to reconstruct images in the compressed sensing framework. Furthermore, by incorporating a grating-based dynamically focused anti-scatter collimator, the SPR can be reduced so that the Trinity system can become clinically relevant. Future work is underway to evaluate real system prototyping, scatter correction, and parametric optimization.

References

[1] W. H. Organization. (2016, 22 Aug). *Cardiovascular diseases (CVDs)*. Available: http://www.who.int/mediacentre/factsheets/fs317/en/

[2] F. Cademartiri, E. Maffei, A. Palumbo, S. Seitun, C. Martini, C. Tedeschi, *et al.*, "Coronary calcium score and computed tomography coronary angiography in high-risk asymptomatic subjects: assessment of diagnostic accuracy and prevalence of non-obstructive coronary artery disease," *European radiology*, vol. 20, pp. 846-854, 2010.

[3] D. Ertel, M. M. Lell, F. Harig, T. Flohr, B. Schmidt, and W. A. Kalender, "Cardiac spiral dual-source CT with high pitch: a feasibility study," *European radiology*, vol. 19, pp. 2357-2362, 2009.

[4] J. Zhao, M. Jiang, T. Zhuang, and G. Wang, "An exact reconstruction algorithm for triple-source helical cone-beam CT," *Journal of X-Ray Science and Technology*, vol. 14, pp. 191-206, 2006.

[5] J. Zhao, Y. Jin, Y. Lu, and G. Wang, "A filtered backprojection algorithm for triple-source helical cone-beam CT," *IEEE transactions on medical imaging*, vol. 28, pp. 384-393, 2009.

[6] H. Hu, "Multi-slice helical CT: scan and reconstruction," *Medical physics*, vol. 26, pp. 5-18, 1999.

[7] E. Sorantin, M. Riccabona, G. Stücklschweiger, H. Guss, and R. Fotter, "Experience with volumetric (320 rows) pediatric CT," *European journal of radiology*, vol. 82, pp. 1091-1097, 2013.

[8] D. Boyd, R. Gould, J. Quinn, R. Sparks, J. Stanley, and W. Herrmmannsfeldt, "A proposed dynamic cardiac 3-D densitometer for early detection and evaluation of heart disease," *IEEE Transactions on Nuclear Science*, vol. 26, pp. 2724-2727, 1979.

[9] C. H. McCollough, R. B. Kaufmann, B. M. Cameron, D. J. Katz, P. Sheedy 2nd, and P. A. Peyser, "Electron-beam CT: use of a calibration phantom to reduce variability in calcium quantitation," *Radiology*, vol. 196, pp. 159-165, 1995.

[10] G. Wang, Y. Liu, Y. Ye, S. Zhao, J. Hsieh, and S. Ge, "Top-level design and preliminary physical analysis for the first electron-beam micro-CT scanner," *Journal of X-Ray Science and Technology*, vol. 12, pp. 251-260, 2004.

[11] R. A. Robb, E. A. Hoffman, L. J. Sinak, L. D. Harris, and E. L. Ritman, "High-speed three-dimensional x-ray computed tomography: The dynamic spatial reconstructor," *Proceedings of the IEEE*, vol. 71, pp. 308-319, 1983.

[12] Y. Cheng, J. Zhang, Y. Z. Lee, B. Gao, S. Dike, W. Lin, *et al.*, "Dynamic radiography using a carbon-nanotube-based field-emission x-ray source," *Review of scientific instruments*, vol. 75, pp. 3264-3267, 2004.

[13] E. M. Quan and D. S. Lalush, "Three-dimensional imaging properties of rotation-free square and hexagonal micro-CT systems," *IEEE transactions on medical imaging*, vol. 29, pp. 916-923, 2010.

[14] G. Cao, Y. Z. Lee, R. Peng, Z. Liu, R. Rajaram, X. Calderon-Colon, *et al.*, "A dynamic micro-CT scanner based on a carbon nanotube field emission x-ray source," *Physics in medicine and biology*, vol. 54, p. 2323, 2009.

[15] H. Yu and G. Wang, "Compressed sensing based interior tomography," *Physics in medicine and biology*, vol. 54, p. 2791, 2009.

[16] H. Gong, H. Yan, X. Jia, B. Li, G. Wang, and G. Cao, "X‐ray scatter correction for multi‐source interior computed tomography," *Medical physics*, vol. 44, pp. 71-83, 2017.

[17] J. A. Meinel, E. Hoffman, A. Clough, and G. Wang, "Reduction of Half-Scan Shading Artifact Based on Full-Scan Correction 1," *Academic radiology*, vol. 13, pp. 55-62, 2006.